Available online at www.sciencedirect.com
ScienceDirect
Journal of Power Sources 174 (2007) 828–831
JOURNAL OF POWER SOURCES
www.elsevier.com/locate/jpowsour

Short communication

Synthesis and electrochemical performance of doped $LiCoO_2$ materials

S.A. Needham [a,*], G.X. Wang [a,b], H.K. Liu [a,b], V.A. Drozd [c], R.S. Liu [c]

[a] *Institute for Superconducting & Electronic Materials, University of Wollongong, Northfields Avenue, Gwynneville, NSW 2522, Australia*
[b] *Australian Research Council Centre of Excellence for Nanostructured Electromaterials, University of Wollongong, Australia*
[c] *National Synchrotron Research Centre, Hsinchu 300, Taiwan*

Available online 3 July 2007

Abstract

Layered intercalation compounds $LiM_{0.02}Co_{0.98}O_2$ ($M = Mo^{6+}$, V^{5+}, Zr^{4+}) have been prepared using a simple solid-state method. Morphological and structural characterization of the synthesized powders is reported along with their electrochemical performance when used as the active material in a lithium half-cell. Synchrotron X-ray diffraction patterns suggest a single phase HT-$LiCoO_2$ that is isostructural to α-$NaFeO_2$ cannot be formed by aliovalent doping with Mo, V, and Zr. Scanning electron images show that particles are well-crystallized with a size distribution in the range of 1–5 μm. Charge–discharge cycling of the cells indicated first cycle irreversible capacity loss in order of increasing magnitude was Zr (15 mAh g^{-1}), Mo (22 mAh g^{-1}), and V (45 mAh g^{-1}). Prolonged cycling the Mo-doped cell produced the best performance of all dopants with a stable reversible capacity of 120 mAh g^{-1} after 30 cycles, but was inferior to that of pure $LiCoO_2$.

Keywords: Lithium cobaltate; Li-ion batteries; Cathode materials; Doped $LiCoO_2$; Solid state synthesis

1. Introduction

Despite increasing research into alternative materials, the layered intercalation compound lithium cobalt oxide ($LiCoO_2$) remains the foundation cathode material used in many commercial lithium ion cells. The theoretical capacity of $LiCoO_2$ is around 274 mAh g^{-1} (i.e., complete lithium delithiation), however the maximum practical capacity achievable is around half of the theoretical value due to a large anisotropic structural change that occurs during the delithiation process [1]. Specifically, when $x = 0.5$ in the Li_xCoO_2 compound, a hexagonal to monoclinic crystallographic phase change occurs which is accompanied by a ∼2.6% volume expansion in *c*-axis. This phenomenon involves cobalt dissolution and is responsible for significant capacity fade and mechanical failure in cells [2,3]. The realized capacity of the $LiCoO_2$ based electrode may be increased by charging beyond 4.2 V, but must also avoid the associated structural change that occurs at higher voltages. Recently, this has been achieved by encapsulating $LiCoO_2$ particles with stable ceramic compounds such as TiO_2, Al_2O_3, and ZrO_2 [4–8], and by novel surface modification techniques [4]. An additional advantage of this technique is related to a "barrier effect" that occurs by the formation of an outer shell, which shields the active $LiCoO_2$ core from the electrolyte and inhibits detrimental side reactions.

Doping is an alternative approach to raise the practical capacity attained by $LiCoO_2$ cathodes. Theoretical studies indicate that transition metal doping of $LiCoO_2$ will result in increased capacity, whereas non-transition metal doping can increase voltage at the expense of capacity [9]. Overall, doping must achieve a solid solution of $LiM_xCo_{1-x}O_2$ that is isostructural with $LiCoO_2$. Significant phase separation could defeat the effect of doping on the potential, and could result in a material with inferior properties compared to the undoped material. The selection of dopant and doping levels should also suppress anisotropic structural change by maintaining interlayer distance. Extensive investigation into cation doping using Ti, Cr, Mn, Fe, Ni, Cu, Zn, Zr, Nb, Rh, Ta, and W is readily available in the literature [10–16]. The underlying trend appears that little success has been achieved by doping $LiCoO_2$ with bi- or tri-valent metal ions, however doping with tetra-valent ions appears more promising. According to Venkatraman et al. [9], these observations have a theoretical basis whereby increasing the valency of the dopant ion (M) produces a higher concentration of Co^{3+} ions and a lower concentration of Co^{4+} ions. The Co^{4+} ion is a Jahn–Teller ion that causes spontaneous deformation in

* Corresponding author. Present address: Dr Scott Needham Manager, Innovation & Commercialisation Materials and Engineering Building 4 - Room 109E University of Wollongong Northfields Ave, NSW 2522, AUSTRALIA.
Tel.: +612 4221 4470; Mob.: 0439 135 268; fax: +61 2 42215731.
E-mail address: scottn@uow.edu.au (S.A. Needham).

0378-7753/$ – see front matter © 2007 Published by Elsevier B.V.
doi:10.1016/j.jpowsour.2007.06.228

CoO_6 octahedra which disrupts the intercalation framework, and reduces capacity. In this report, we present the synthesis and electrochemical performance of $LiCoO_2$ doped with Mo^{6+}, V^{5+}, and Zr^{4+} ions prepared powder from a solid-state method. To our knowledge, there is no literature on the synthesis and electrochemical performance of $LiCoO_2$ doped with Mo^{6+} and V^{5+} ions. From a commercial viewpoint, the selective doping of $LiCoO_2$ powders produced by an easily scalable solid-state process offers a viable solution to increase the stability and capacity of $LiCoO_2$.

2. Experimental

$LiM_{0.02}Co_{0.98}O_2$ [M = Mo, V, Zr] powders were prepared in separate experiments using Li_2CO_3 (>99.9%), Co_3O_4 (99.9%), and either Mo_2O_3 (99.5%), V_2O_3 (99%) or ZrO_2 (99.5%) reagents all sourced from Aldrich. Stoichiometric quantities were wet mixed in an agate mortar using ethanol to form a paste and dried in a vacuum oven at 150 °C for 2 h. Precursors were ground and transferred to alumina boats for annealing at 850 °C for 12 h, then cooled to ambient temperature, reground and annealed for 12 h. Analysis of the composition and crystal structure of the powders was conducted using a Philips PW1730 X-ray diffractometer with monochromatised Cu Kα radiation (λ = 1.5418 Å) at a scan rate of 2 min^{-1}. Further structural analysis was conducted *via* synchrotron radiation (λ = 0.516606 Å) experiments at the National Synchrotron Research Centre, Taiwan. The morphology of the powders was observed by a JEOL JSM-6460A scanning electron microscope (SEM). Electrochemical measurements were conducted by assembly of standard R2032 coin-type cells. Working electrodes were constructed by mixing 75 wt% active powder, 15 wt% carbon black (Lexel, 99%), and 10 wt% polyvinylidene fluoride (Aldrich, 99%) in a mortar and pestle. The dry powder mix was blended with *N*-methylpyrrolidinone to make a slurry, which was then spread uniformly on 1 cm^2 by 0.1 mm thick aluminum foil (99.99%) substrate. The electrodes were dried in a vacuum oven for 12 h at 80 °C then cold pressed at 300 kg cm^{-2} in a uniaxial hydraulic press. All electrodes contained no more than 2 mg of active material and were assembled into a test coin cell in a high purity argon-filled glove-box (Mbraun, Unilab, USA) where the concentration of H_2O < 5 ppm and O_2 < 10 ppm. Battery grade lithium foil was used as both the counter and reference electrodes. Celgard® 2400 (Celgard LLC, USA) was used as a separator membrane soaked in a 1 M of $LiPF_6$ dissolved in a 1:1 by volume mixture of ethylene carbonate (EC) and dimethyl carbonate (DMC) electrolyte (MERCK KgaA, Germany). Charge–discharge cycles of the half-cells were measured from 3.0 to 4.2 V versus Li/Li^+ at C/15 (1C = 140 mAh g^{-1}) using a battery cycler (Neware) in galvanostatic mode. Specific capacity was calculated based on the mass of active material in the electrode. Cyclic voltammograms (CV) were obtained by measuring the current–voltage (I–V) response at a scan rate of 0.02 mV s^{-1} from 3.0 to 4.5 V using an electrochemical workstation (CHI Instruments, model 660A). All electrochemical testing was carried out at ambient temperature (23 ± 2 °C).

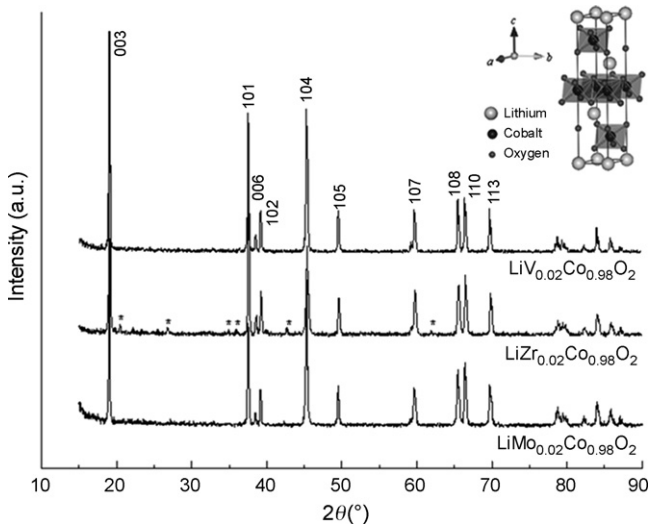

Fig. 1. X-ray diffraction patterns of $LiM_{0.02}Co_{0.98}O_2$ powders with M = Mo, Zr, V. Secondary phase in the $LiZr_{0.02}Co_{0.98}O_2$ powder is indexed to Li_2ZrO_3 (*).

3. Results and discussion

Fig. 1 shows the X-ray diffraction patterns of the as synthesized $LiM_{0.02}Co_{0.98}O_2$ for M = Mo, Zr, V and a schematic projection of the indexed hexagonal unit cell of pure $LiCoO_2$. All major peaks are clearly identifiable to HT-$LiCoO_2$, which is isostructural to layered α-$NaFeO_2$ with an $R-3m$ space group. In this structure, the constituent atoms Co, Li, and O occupy the 3a, 3b, and 6c Wychoff sites, respectively. All diffraction patterns also show that the (0 0 6)–(1 0 2) and (1 0 8)–(1 1 0) peak doublets are well defined and separated. This suggests a dimensionally stable structure with a highly ordered distribution of cations in the lattice [17]. Further evidence of cation ordering is indicated by the ratio of (0 0 3) and (1 0 4) peak intensities (I_{003}/I_{104}) exceeding unity, which is commonly observed in pristine $LiCoO_2$. Clear evidence of a secondary phase in the Zr-doped powder has been indexed to monoclinic structure Li_2ZrO_3 (ICDD 16-0263) with a $C2/c$ space group [18]. Minor amounts of secondary phases in the Mo and V-doped powders were identified synchrotron radiation XRD experiments. Values of the refined unit cell parameters from the Rietveld analysis of synchrotron XRD patterns are given in Table 1 for all compositions. The χ^2, R_p (profile), and R_{wp} (weighted pattern) factors are included and indicate the quality of the Rietveld refinements. The lattice parameter a indicates the intralayer metal–metal distance, and c is the inter slab distance. The values of a and c

Table 1
Unit cell parameters and the c/a ratio for $LiM_{0.02}Co_{0.98}O_2$ powders

Parameter	Mo	V	Zr
Composition	$LiCoO_2$; molybdates	$LiCoO_2$; Li_3VO_4	$LiCO_2$; Li_2ZrO_3
a (Å)	2.8136(3)	2.8159(3)	2.8102(3)
c (Å)	14.0487(2)	14.0551(2)	14.0443(2)
c/a ratio	4.993	4.991	4.998
R_p (%)	4.52	4.75	4.86
R_{wp} (%)	6.68	7.58	7.95
χ^2	0.9404	1.011	1.056

for pure $LiCoO_2$ are 2.809 and 14.037 Å, respectively, which are in good agreement with data previously reported [19]. The results from $LiM_{0.02}Co_{0.98}O_2$ powders show that both the *a* and *c* parameters are the highest in the Mo and V-doped powders and represent a general increase the unit cell parameters compared to pristine $LiCoO_2$. On the other hand, the Zr-doped powders show no change in the unit cell parameters compared to pristine $LiCoO_2$ within the limits of experimental error. These results may be interpreted by comparing the ionic radius substituted Co^{3+} ion (0.65 Å) to the dopant elements; V^{5+} (0.4 Å) < Mo^{6+} (0.65 Å) < Zr^{4+} (0.87 Å). By substituting elements with a smaller ionic radii (V^{5+}), the unit cell usually contracts. However, if these ions are located in the interstitices, a reduction in unit cell parameters may not be observed. Our result therefore confirms that V primarily did not replace Co in vacant 3a sites, but rather existed elsewhere within the structure as a secondary phase. In the opposite case, by substituting an element with larger ionic radii (Zr^{4+}) often leads to expansion of the unit cell parameters and overall cell volume. The absence of unit cell expansion in our Zr-doped powder was due to Zr forming a secondary Li_2ZrO_3 phase, rather than substituting for Co in the vacant 3a Wychoff site.

It should also be noted in Table 1 that another indication of cation order/disorder and the metal–metal layer distance can be discerned from the *c*/*a* ratio. For a cation-disordered rock salt structure, we know that the *c*/*a* ratio should be 4.899 or lower which produces a face centred unit cell (Fd3m) with a spinel structure [20]. All $LiM_{0.02}Co_{0.98}O_2$ and pristine $LiCoO_2$ powders as assessed by the *c*/*a* ratio do not indicate significant cation disorder within the $LiCoO_2$ lattice.

Fig. 2 shows a typical SEM of the as-synthesized powders. All $LiM_{0.02}Co_{0.98}O_2$ powders appear consistent with those prepared by solid-state methods in other works [1]. Particles are well crystallized with a broad size distribution in the range of 1–5 μm.

Cyclic voltammograms of the $LiM_{0.02}Co_{0.98}O_2$ cells in the second cycle are shown in Fig. 3. Broad and smooth curves in the anodic and cathodic I–V plots indicate either a second-order phase transition or continuous single-phase reactions with

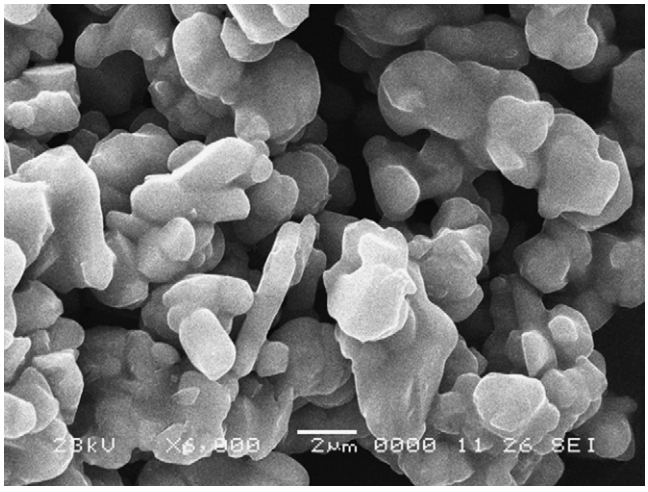

Fig. 2. A typical SEM image of $LiM_{0.02}Co_{0.98}O_2$ powders.

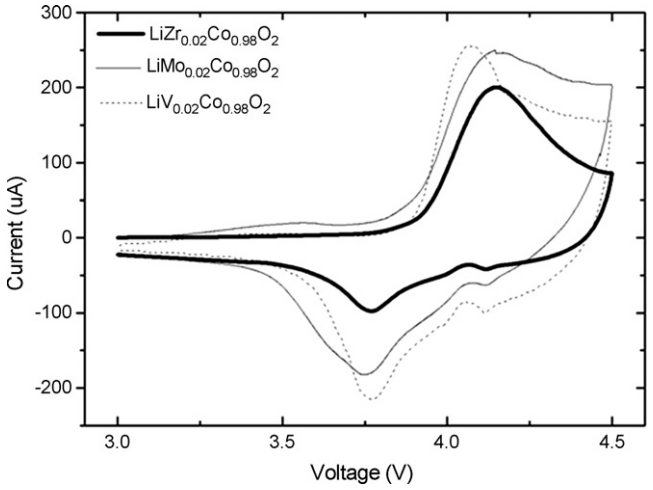

Fig. 3. Cyclic voltammograms of $LiM_{0.02}Co_{0.98}O_2$ cells at a scan rate of 0.02 mV s^{-1} between 3.0 and 4.5 V.

lithium ions in the oxide materials. In our plots, the primary oxidation (4.05 V) and reduction peaks (3.75 V) represent lithium deintercalation and intercalation into the active host respectively, and are characteristic of hexagonal phase in these layered compounds. Two additional secondary peaks situated roughly at 4.05 and 4.2 V can also be seen during reduction. The presence of these peaks has been previously reported [10,21], and corresponds to the well-known hexagonal-monoclinic crystallographic phase transformation occurring at $x = 0.5$ in Li_xCoO_2. Overall, observed features are in good agreement with the I–V behavior reported in the literature [22,23] and indicate that the charge/discharge process occurs in a reversible manner in the voltage scanning region of 3.0–4.5 V versus Li/Li^+.

The electrochemical performance of coin cells were evaluated by galvanostatic cycling from 3 to 4.2 V at C/15 (1C = 140 mAh g^{-1}) over 30 cycles (Fig. 4). Cells exhibited an open circuit potential between 2.7 and 3.2 V versus Li/Li^+.

All cells exhibit a high first charge in the range of 160 mAh g^{-1}, with the extent of the irreversible capacity loss between the first charge and first discharge highly dependant

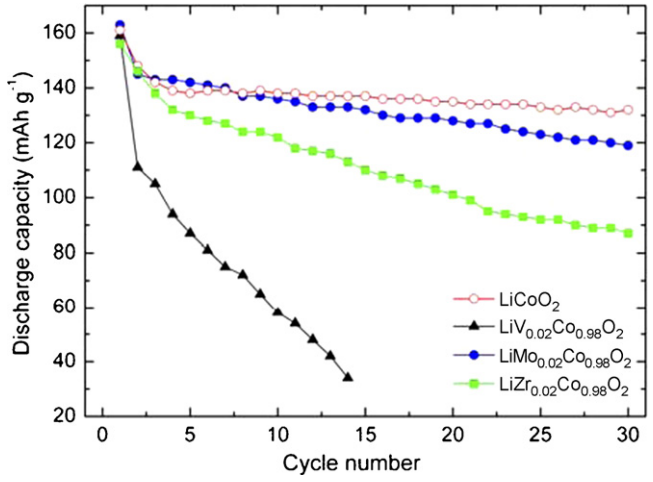

Fig. 4. Galvanostatic cycling of $LiM_{0.02}Co_{0.98}O_2$ and $LiCoO_2$ reference electrodes at C/15 between 3.0 and 4.2 V.

upon the type of metal ion dopant. The irreversible capacity loss in order of increasing magnitude was Zr (15 mAh g^{-1}), Mo (22 mAh g^{-1}), and V (45 mAh g^{-1}). The rate of capacity fade over 30 cycles was also extremely varied between the metal dopants. Cycling the V-doped cell led to rapid capacity fading and complete failure in less than 15 cycles. The Zr-doped cell produced moderate capacity fade, resulting in a capacity of 85 mAh g^{-1} after 30 cycles. However, the best performance amongst doped cells was achieved by Mo doping, which recorded a reversible capacity of 120 mAh g^{-1} after 30 cycles. Jin et al. [24] have linked the presence of secondary phases in $LiCoO_2$ to improved cyclability of $LiCoO_2$-based electrodes. In that report, commercial $LiCoO_2$ powders were surface modified with the second phase, which suppressed the reaction between the Co^{4+} and the electrolyte. In our case, it is not expected that the secondary phases would exist as a continuous coating on the surface of the $LiCoO_2$ particles, and therefore it would not provide any barrier effect between particles and the electrolyte. The formation of secondary phases would however result in a lithium deficient $LiCoO_2$ structure that contains a higher concentration of Co^{4+} compared to the un-doped powder.

4. Conclusions

Careful structural characterization of doped $LiCoO_2$ compounds by synchrotron X-ray diffraction confirmed that some quantity of secondary phases formed in all cases. The presence of these random secondary phases disrupts the $LiCoO_2$ structure and is thought to effect the electronic structure by increasing the concentration of Co^{4+} ions. Work is underway to further investigate the electronic structure of the prepared materials. Clearly, the electrochemical properties of the materials investigated have been adversely affected by the formation of these secondary phases.

Acknowledgements

The authors would like to acknowledge financial support provided by the Australian Research Council (ARC) through ARC linkage project LP0453766 and the Centre of Excellence program. Assistance from Mr. Alan Richards from Bluescope Steel concerning X-ray diffraction analysis is also greatly appreciated.

References

[1] R. Alcantara, P. Lavela, J.L. Tirado, J. Solid State Chem. 134 (1997) 265.
[2] G. Ceder, Y.-M. Chiang, D.R. Sadoway, M.K. Aydinol, Y.-I. Jang, B. Huang, Nature 392 (1998) 694.
[3] G.G. Amatucci, J.M. Tarascon, L.C. Klein, Solid State Ionics 83 (1996) 167.
[4] S.-M. Park, T.-H. Cho, Y.-M. Kim, M. Yoshio, Electrochem. Solid State Lett. 8 (6) (2005) A299.
[5] Z. Chen, J.R. Dahn, Electrochem. Solid State Lett. 5 (10) (2002) A213.
[6] J. Cho, Y.J. Kim, T.-J. Kim, B. Park, Angew. Chem. Int. Ed. 40 (18) (2001) 3367.
[7] J. Cho, Y.J. Kim, T.-J. Kim, B. Park, Chem. Mater. 12 (2000) 3788.
[8] J. Cho, Y.J. Kim, T.-J. Kim, B. Park, J. Electrochem. Soc. 148 (A11) (2001) A1110.
[9] S. Venkatraman, V. Subramanian, S. Gopu Kumar, N.G. Renganathan, N. Muniyandi, Electrochem. Commun. 2 (2000) 18.
[10] S. Gopukumar, Y. Jeong, K.-B. Kim, Solid State Ionics 159 (2003) 223.
[11] M. Zou, M. Yoshio, S. Gopukumar, J.-I. Yamaki, Chem. Mater. 17 (6) (2005) 1284.
[12] M. Zou, M. Yoshio, S. Gopukumar, J.-I. Yamaki, Chem. Mater. 15 (25) (2003) 4699.
[13] H.-S. Kim, T.-K. Ko, B.-K. Na, W.-I. Cho, B.-W. Chao, J. Power Sources 138 (2004) 232.
[14] S.-H. Oh, S.-M. Lee, W.-I. Cho, B.-W. Cho, Electrochim. Acta 51 (18) (2006) 3637.
[15] C.D. Jones, E. Rossen, J.R. Dahn, Solid State Ionics 68 (1994) 65.
[16] Y. Toyoguchi, European Patent Application 90106149.9 (1990) [filed March 30, 1990, published October 10, 1990].
[17] H. Wang, Y.I. Jang, B. Huang, D.R. Sadoway, Y.M. Chiang, J. Electrochem. Soc. 146 (1999) 473.
[18] H.M. Rietveld, J. Appl. Crystallogr. 2 (1969) 65.
[19] S.M. Lala, L.A. Montoro, V. Lemos, M. Abbate, J.M. Rosolen, Electrochim. Acta 51 (2005) 7.
[20] E. Rossen, J.N. Reimers, J.R. Dahn, Solid State Ionics 62 (1993) 53.
[21] J.N. Reimers, J.R. Dahn, J. Electrochem. Soc. 139 (1992) 2091.
[22] Y.-M. Choi, S.-I. Pyun, Solid State Ionics 99 (1997) 173.
[23] B. Huang, Y.-I. Jang, Y.-M. Chiang, D.R. Sadoway, J. Appl. Electrochem. 28 (1998) 1365.
[24] Y. Jin, N. Li, C.H. Chen, S.Q. Wei, Electrochem. Solid State Lett. 9 (6) (2006) A273.